J Mater Sci (2010) 45:2390–2402
DOI 10.1007/s10853-010-4205-1

Effects of heat treatment process and niobium addition on the microstructure and mechanical properties of low carbon steel weld metal

Shanping Lu · Shitong Wei · Dianzhong Li · Yiyi Li

Received: 16 April 2009 / Accepted: 2 January 2010 / Published online: 20 January 2010

Abstract The mechanical properties and microstructure were evaluated and analyzed by optical microscopy (OM) and transmission electron microscopy (TEM) for microalloy carbon steel weld metal with and without Nb addition, respectively, under different heat treatment processes including stress relief annealing, normalizing, and no treatment after welding. The strength and elongation of the weld metal without treatment after welding were improved with the addition of Nb element, and the impact toughness was not affected obviously with the Nb addition. After stress relief annealing, the strength decreased for the Nb-free weld metal, while the elongation and impact toughness increased. However, for the Nb-bearing weld metal, stress relief annealing improved the strength of the weld metal significantly, and deteriorated the elongation and impact toughness. In the case of normalizing treatment to the weld metal, it was shown that with the increase of the holding time at the normalizing temperature of 920 °C, for both the weld metals with and without Nb addition, the microstructure of the columnar grain zone (CGZ) was transformed from one of columnar grain into one of equiaxed grain. The grain size of the equiaxed grain zone (EGZ) increased initially, then remained almost unchanged with the prolonging of the holding time. The mechanical properties of the weld metal with and without Nb addition showed no obvious change with the increasing holding time. With the increase of the normalizing temperature, the strength of the Nb-bearing weld metal increased, while the elongation and impact toughness decreased significantly. OM and TEM analysis found that the fine NbC particles were precipitated at the normalizing temperature of 920 °C, which refined the grains of the weld metal and increased the impact toughness. With the increase of the normalizing temperature, the content of widmanstatten ferrite (WF) in the Nb-bearing weld metal increased, whereas the quantity of the NbC particles decreased, which improved the strength and lowered the impact toughness.

S. Lu (✉) · S. Wei · D. Li · Y. Li
Shenyang National Laboratory for Materials Science, Institute of Metal Research, Chinese Academy of Sciences, 72 Wenhua Road, Shenyang 110016, People′s Republic of China
e-mail: shplu@imr.ac.cn; weist2003@yahoo.com.cn

Introduction

Niobium, vanadium, and titanium have a great atomic affinity for carbon atom, and can greatly form MC carbide with high hardness, high melting point, and very good stability. The mechanical properties of low carbon steel can be improved through single or combined addition of Nb, V, or Ti. One important characteristic of these microalloy elements is that they can dissolve into the substrate at proper temperature, and precipitate carbide as the temperature decreases during the hot working and cooling process. The precipitates have great influence on the microstructure and mechanical properties of steels. A small addition of microalloy elements to low carbon steels is very effective in restraining the growth of austenite grain and inhibiting austenite recrystallization [1–4]. At present, Nb element is widely used in the production of microalloy steel. It has the effects of grain refinement and precipitation hardening as solute Nb atoms or NbC precipitates. Nb is one of the most effective elements for improving the strength and toughness of the steels [5–8]. Adjusting the Nb element content can change C partition in carbide and substrate, thus controlling the steel microstructure and mechanical properties. The content of niobium is usually higher than 0.02% in the niobium steels for forming precipitates of NbC particles [9].

Nb microalloyed steel is one of the important structure materials. Welding is one of the material processing methods for structural matals having potential applications in the industrial area. Many previous studies concerning Nb steels had focused on the transformation behavior in thermomechanical process and the effect of Nb element on the process [10–16], as well as the effect of solute Nb on the microstructure and properties of weld metal before and after stress relief annealing [17–24]. However, it was seldom reported about the effect of normalizing treatment at higher temperatures above the transformation temperature on the microstructure and properties of Nb-bearing weld metal. In addition, the precipitates distribution situations in the Nb-bearing weld metals under different post-weld heat treatment processes were also less discussed in the previous articles. In this study, Nb was used as the main carbide-forming element in the weld metal. The effect of Nb on the microstructure, tensile properties, and impact toughness of C–Mn–Si steel weld metal under different post-weld heat treatment processes was investigated systematically, and the mechanism was also discussed. The research provided theoretical guidance for the design of low alloy steel welding materials and property controlling of weld metal.

Experimental procedures

Two kinds of welding wires with the diameter of 1.2 mm (welding wire 1 without Nb, welding wire 2 with 0.06% Nb) were used in the experiment to weld the 12-mm thick S355J2G3 (base metal) steel plate by automatic Gas Metal Arc Welding (GMAW). Table 1 gives the chemical compositions of the welding wires and base metal. Except for the Nb element, the contents of other elements in these two welding wires are almost the same. Figure 1 shows the schematic diagram of the Y-type joint by three-pass welding, and the first pass is the back sealing welding. The shielding gas is composed of 85%Ar + 15%CO_2. The chemical compositions of the weld metals deposited by welding wires 1 and 2 were analyzed using chemistry analysis and shown in Table 2. After welding, different heat treatment processes were carried out to the welded plates including annealing and normalizing at different parameters as shown in Table 3.

Tensile tests of weld metal were conducted at room temperature using computerized tensile testing system on an Instron-type testing machine. The weld metal consists of columnar grain zone (CGZ) and equiaxed grain zone (EGZ) (it experiences the normalizing process by the subsequent welding bead) as multipass welding is used.

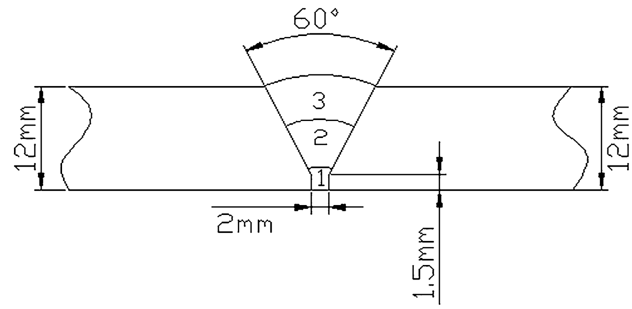

Fig. 1 The schematic diagram of welded joint

Table 2 Chemical compositions of the weld metals (wt%)

Welding wire used	C	Si	Mn	P	S	Nb
Welding wire 1	0.080	0.73	1.40	0.009	0.010	–
Welding wire 2	0.078	0.70	1.38	0.009	0.008	0.048

Table 3 Heat treatment processes and the states of the joints

Number	Heat treatment processes and the states of the joints
0	As-welded
1	Annealing at 590 °C for 3 h
2	Normalizing at 920 °C for 0.5 h
3	Normalizing at 920 °C for 2 h
4	Normalizing at 920 °C for 3.5 h
5	Normalizing at 920 °C for 5 h
6	Normalizing at 1020 °C for 2 h
7	Normalizing at 1120 °C for 2 h
8	Normalizing at 1200 °C for 2 h

Table 1 Chemical compositions of base material and welding wires (wt%)

Material	C	Si	Mn	S	P	Cu	Nb	Cr	Ni	Al
Base metal	0.14	0.18	1.10	0.0016	0.014	0.012	0.019	0.028	0.026	0.031
Welding wire 1	0.072	0.88	1.54	0.006	0.007	0.071	–	–	–	–
Welding wire 2	0.068	0.94	1.52	0.004	0.008	0.082	0.060	–	–	–

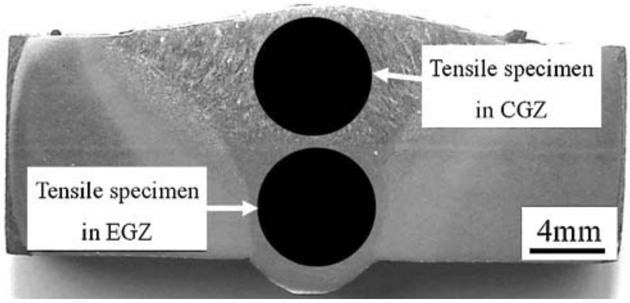

Fig. 2 The schematic diagram of the tensile specimen positions in CGZ and EGZ of weld metal

The tensile tests were conducted on both the CGZ and EGZ, and the respective tensile specimens were cut from the CGZ and EGZ of the weld metal along the welding direction as shown in Fig. 2. The specimens for impact property test of weld metal were extracted from these joints transversely to the welding direction using an electrical spark wire cutting machine and were machined to a dimension of 55 mm × 10 mm × 10 mm. The V notch was machined in the center of the weld metal on the cross section of the joints. The impact tests were examined on the swing impacting test machine at −20 °C. All the mechanical properties tests were done three times, and the average values were calculated. The microstructures of the weld metal were observed by using optical microscopy. Transmission electron microscopy and selected area diffraction (SAD) pattern were used to directly observe and analyze the precipitates in the carbon extraction replicas of the weld metal with Nb addition. Carbon extraction replicas were prepared by etching the polished surface in 2% natal, coating the surface with a thin film of carbon, then stripping the film, and cleaning in acetone. Specimens were examined by means of JEM 2010 operated at 200 kV.

Results

Mechanical properties

As-welded and as-annealed states

The average yield strength, tensile strength, elongation, and −20 °C impact energy of the weld metal without and with Nb addition at as-welded and as-annealed (590 °C for 3 h) states are presented in Tables 4 and 5. The as-welded Nb-free weld metal has lower yield and tensile strengths, elongation and equivalent −20 °C impact energy comparing with those of the as-welded Nb-bearing weld metal. After annealing technology, the yield and tensile strengths of the Nb-free weld metal decreased, while the elongation and −20 °C impact energy increased, as shown in Table 4. For the Nb-bearing weld metal, after annealing process, the yield and tensile strengths increased, the elongation and −20 °C impact energy decreased, as shown in Table 5. In order to explain this phenomenon, the analysis of the microstructure of the weld metal with Nb addition is necessary.

Normalizing state

Mechanical properties of the weld metal with and without Nb addition under different normalizing conditions are shown in Figs. 3 and 4. When the normalizing temperature was set at 920 °C, the yield strength, tensile strength, elongation, and −20 °C impact energy of the Nb-bearing weld metal were all higher than those of the Nb-free weld metal, and these values were changed only slightly with the increase of the holding time from 0.5 to 5 h, as shown in Fig. 3a–d, respectively.

The yield strength, tensile strength, elongation, and −20 °C impact energy of the Nb-free weld metal changed slightly with the increase of the normalizing temperature as

Table 4 Mechanical properties of the as-welded and as-annealed weld metal without Nb addition

State	Sampling location	Yield strength (MPa)	Tensile strength (MPa)	Elongation (%)	−20 °C impact energy (J)
As-welded	CGZ	425	570	26.0	46
	EGZ	368	542	33.3	
As-annealed	CGZ	400	540	28.0	108
	EGZ	362	524	34.7	

Table 5 Mechanical properties of the as-welded and as-annealed weld metal with Nb addition

State	Sampling location	Yield strength (MPa)	Tensile strength (MPa)	Elongation (%)	−20 °C impact energy (J)
As-welded	CGZ	505	640	27.0	46
	EGZ	439	600	35.3	
As-annealed	CGZ	610	705	22.0	26
	EGZ	501	631	25.3	

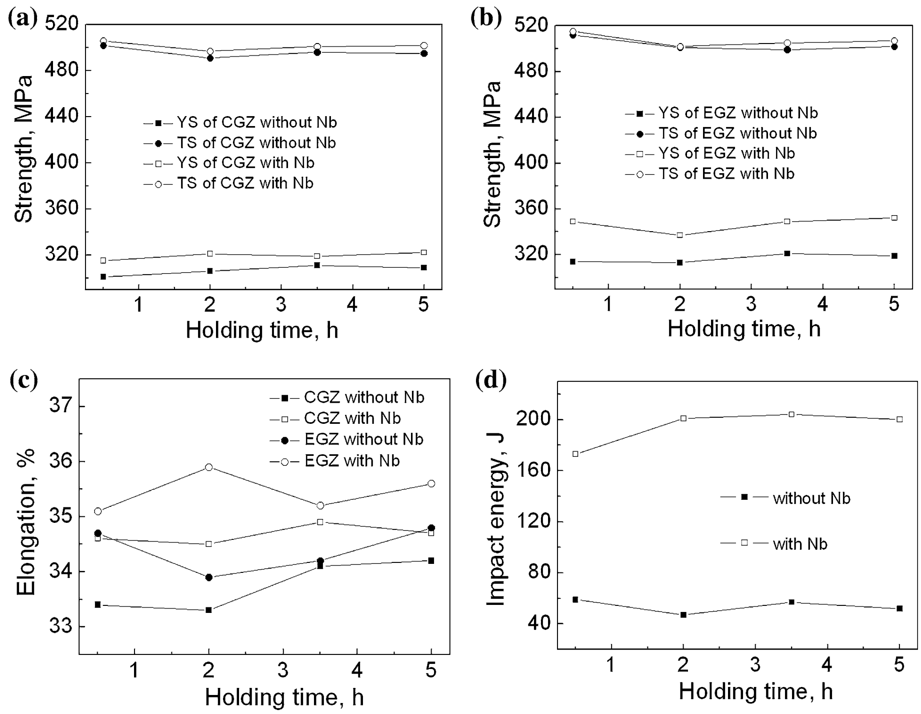

Fig. 3 Effect of normalizing holding time on the properties of weld metal with and without Nb: **a** strength of the CGZ, **b** strength of the EGZ, **c** elongation, **d** impact energy

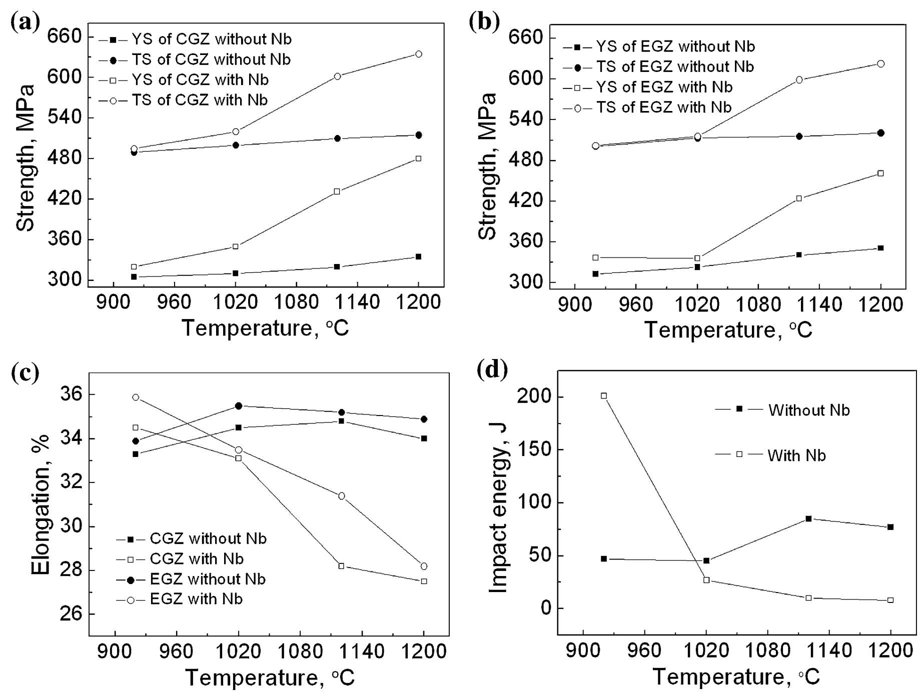

Fig. 4 Effect of normalizing temperature on the properties of weld metal with and without Nb: **a** strength of the CGZ, **b** strength of the EGZ, **c** elongation, **d** impact energy

shown in Fig. 4a–d, respectively. However, for the Nb-bearing weld metal, the yield and tensile strengths increased obviously (Fig. 4a, b), while the elongation and −20 °C impact energy decreased significantly (Fig. 4c, d) with the increasing normalizing temperature. When the normalizing holding time was kept at 2 h and the temperature was raised to 920, 1020, 1120 and 1200 °C, the corresponding yield and tensile strengths of the Nb-bearing weld metal were all higher than those of the Nb-free weld metal as shown in Fig. 4a, b. When the normalizing temperatures was 920 °C, the elongation and −20 °C impact energy of the Nb-free weld metal were lower than those of the Nb-bearing weld metal, but when the normalizing temperature was raised to 1020, 1120, and 1200 °C, the elongation and −20 °C impact energy of the Nb-free weld metal would exceed the values of the Nb-bearing weld metal (Fig. 4c, d).

Microstructure

As-welded and as-annealed states

Figure 5 shows the typical macrograph on the cross section of the multipass welding joint composed of weld metal (WM) with CGZ and EGZ, heat affected zone (HAZ), and base metal (BM). The CGZ and EGZ of weld metal could be distinguished obviously. The optical microstructure of CGZ and EGZ is presented in Fig. 6. The CGZ of the as-welded weld metal consists of widmanstatten ferrite (WF), pro-eutectoid ferrite (PF), acicular ferrite (AF), and minor pearlite (P) as shown in Fig. 6a, b. Small addition of Nb element increases the WF and AF contents and decreases the PF proportion in the CGZ of weld metal as a comparison of Fig. 6a with b shows. The EGZ of the as-welded weld metal consists of equiaxed ferrite and minor pearlite as shown in Fig. 6c, d. The EGZ grain size for Nb-bearing weld metal (Fig. 6d) is smaller than that of the Nb-free weld metal (Fig. 6c), due to the effect of Nb element. The optical microstructure of weld metal at as-annealed (590 °C for 3 h) state has no obvious difference from the microstructure at the as-welded state due to the lower heat treatment temperature.

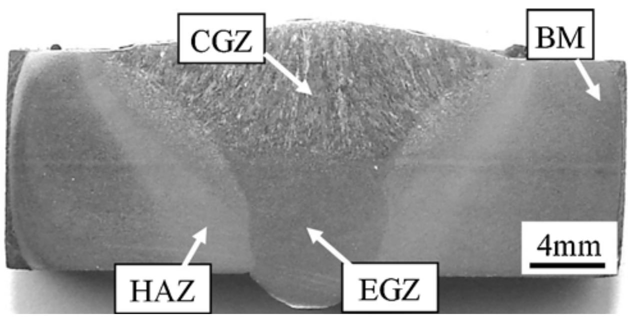

Fig. 5 Macrograph on cross section of the multipass welding joint

TEM was used to directly observe the precipitates in the carbon extraction replicas of the Nb-bearing weld metal at as-welded and as-annealed states, as shown in Fig. 7. No precipitate was found in the CGZ of the as-welded weld metal (Fig. 7a), while some precipitates were observed in the EGZ of the as-welded weld metal (Fig. 7b). After annealing process, fine precipitates were observed in the CGZ and EGZ of the Nb-bearing weld metal as shown in Fig. 7c, d. The precipitates formed in the annealing process were smaller than those formed in the EGZ of the as-welded weld metal (Fig. 7b). SAD analysis was used, and the precipitates were confirmed to be the NbC particles with fcc structure as shown in Fig. 7e.

Normalizing state

The optical microstructures of CGZ and EGZ for the weld metal with or without Nb addition at different normalizing

Fig. 6 Microstructure of weld metal at as-welded state: **a** CGZ of weld metal without Nb, **b** CGZ of weld metal with Nb, **c** EGZ of weld metal without Nb, **d** EGZ of weld metal with Nb

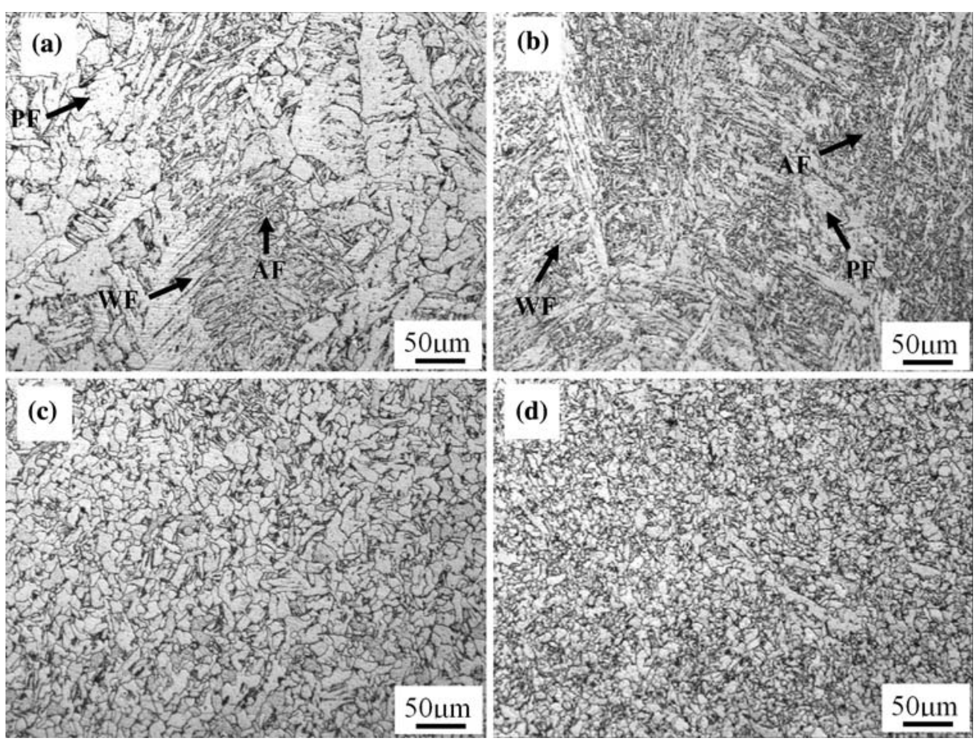

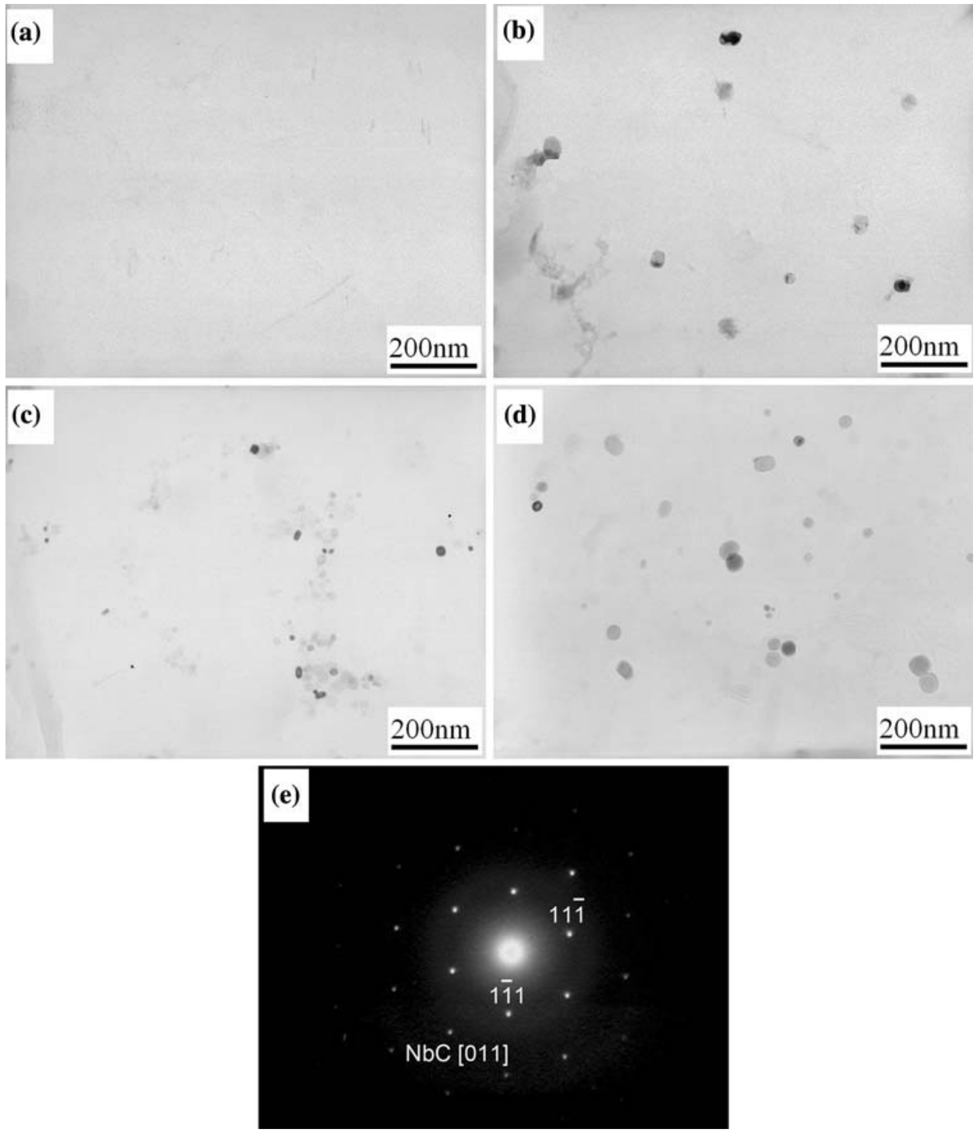

Fig. 7 TEM micrographs of weld metal with Nb and SAD pattern analysis of precipitates: **a** CGZ at the as-welded state, **b** EGZ at the as-welded state, **c** CGZ at the as-annealed state, **d** EGZ at the as-annealed state, **e** SAD pattern analysis of precipitates

conditions are presented in Figs. 8, 9, 10, and 11. Figures 8 and 9 show the microstructure development of CGZ and EGZ of weld metal normalized at 920 °C for different normalizing holding times. After normalizing at 920 °C for 0.5 h, the WF disappeared and the microstructure of the CGZ transformed into equiaxed ferrite and pearlite, but the as-welded columnar structure orientation still retained the characteristic of incomplete normalizing structure due to the short holding time (Fig. 8a, b). With the prolonging of normalizing holding time to 2 h at 920 °C, the as-welded columnar structure orientation in the CGZ disappeared completely (Fig. 8c, d). The CGZ of the weld metal presented the complete normalizing structure because of the relatively long holding time. The ferrite changed from columnar crystal of the as-welded state to equiaxed grains. Both the weld metal with and without Nb addition were composed of equiaxed ferrite and pearlite with the similar grain size. When the holding time was further prolonged to 3.5 and 5 h at 920 °C, the ferrite grains in the CGZ of the weld metal were not obviously grown comparing with the microstructure treated at 920 °C for 2 h (Fig. 8e–h).

Figure 9 shows the microstructure development of the EGZ under the normalizing condition of 920 °C for different normalizing holding times. The grain size in the EGZ of the Nb-bearing weld metal was obviously smaller than the grain size in the EGZ of the Nb-free weld metal. After normalizing at 920 °C for 0.5 h, the grain size in EGZ of the Nb-free weld metal grown up (Fig. 9a) comparing with the as-welded state (Fig. 6c), while the grain size in EGZ of the Nb-bearing weld metal remained almost unchanged (Fig. 9b) compared with the as-welded microstructure shown in Fig. 6d. When the normalizing holding time was prolonged to 2 h at 920 °C, the grain size in the EGZ of the weld metal was larger than that at the

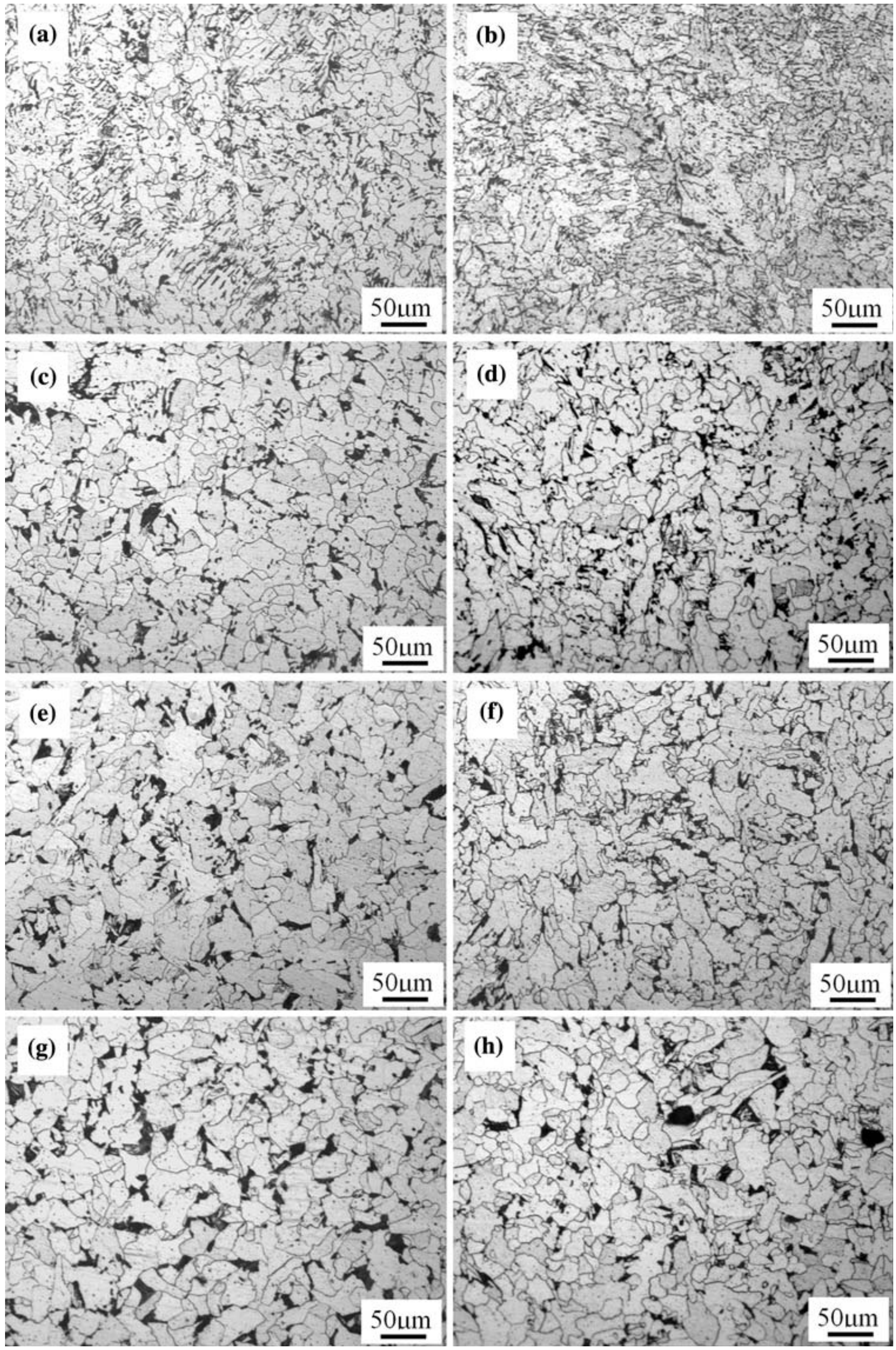

Fig. 8 Microstructure of CGZ for weld metal normalizing at 920 °C for different holding times: **a** weld metal without Nb for 0.5 h, **b** weld metal with Nb for 0.5 h, **c** weld metal without Nb for 2 h, **d** weld metal with Nb for 2 h, **e** weld metal without Nb for 3.5 h, **f** weld metal with Nb for 3.5 h, **g** weld metal without Nb for 5 h, **h** weld metal with Nb for 5 h

normalizing condition of 920 °C for 0.5 h (Fig. 9c, d). When the holding time was further prolonged to 3.5 and 5 h at 920 °C, the ferrite grains in the EGZ of the weld metal were not obviously grown compared with the microstructure treated at 920 °C for 2 h (Fig. 9e–h).

Figures 10 and 11 show that the grain size of the Nb-bearing weld metal (Figs. 10b, d, f, h and 11b, d, f, h) increases more obviously than that of the Nb-free weld metal (Figs. 10a, c, e, g and 11a, c, e, g) with the increase of the normalizing temperature. For the Nb-bearing weld metal, the WF content, in both the CGZ and EGZ, increased with the increasing normalizing temperature as shown in Figs. 10b, d, f, h and 11b, d, f, h. When the normalizing temperature rose from 920 to 1020 °C, partial

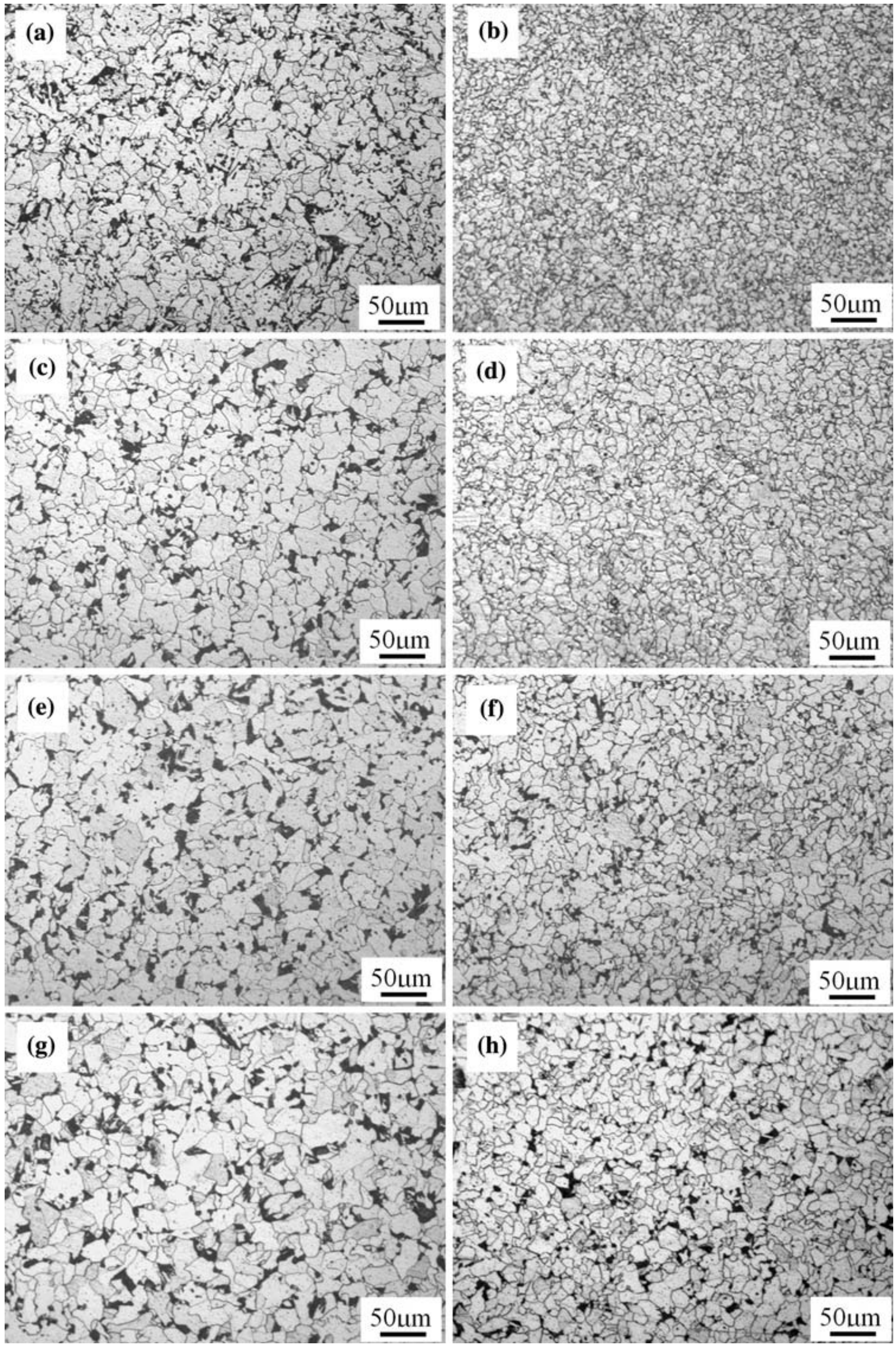

Fig. 9 Microstructure of EGZ for weld metal normalizing at 920 °C for different holding times: **a** weld metal without Nb for 0.5 h, **b** weld metal with Nb for 0.5 h, **c** weld metal without Nb for 2 h, **d** weld metal with Nb for 2 h, **e** weld metal without Nb for 3.5 h, **f** weld metal with Nb for 3.5 h, **g** weld metal without Nb for 5 h, **h** weld metal with Nb for 5 h

WF was observed in the CGZ of the Nb-bearing weld metal (Fig. 10d), but no WF was formed in the CGZ of the Nb-free weld metal (Fig. 10c). More WF was formed in the CGZ of the Nb-bearing weld metal with the increase of the normalizing temperature (Fig. 10f, h), No WF was found in the CGZ of the Nb-free weld metal at the normalizing condition of 1120 °C for 2 h (Fig. 10e). When the normalizing temperature was raised to 1200 °C, the majority of the CGZ of the Nb-bearing weld metal changed into WF, while the others converted into equiaxed ferrite (Fig. 10h). However, only a little WF was observed in the CGZ of the Nb-bearing weld metal (Fig. 10g).

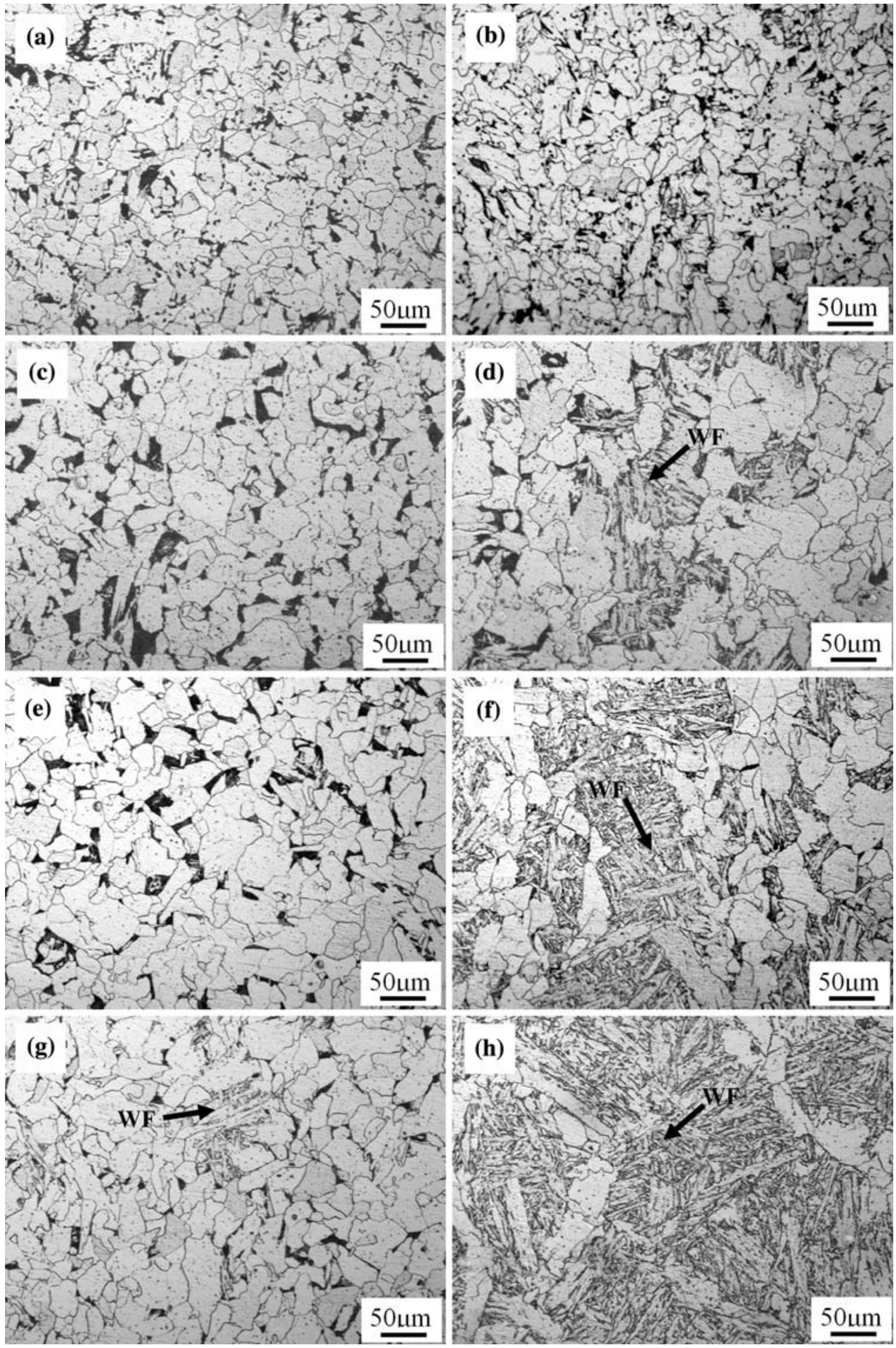

Fig. 10 Microstructure of CGZ for weld metal at different normalizing temperatures for 2 h: **a** weld metal without Nb at 920 °C, **b** weld metal with Nb at 920 °C, **c** weld metal without Nb at 1020 °C, **d** weld metal with Nb at 1020 °C, **e** weld metal without Nb at 1120 °C, **f** weld metal with Nb at 1120 °C, **g** weld metal without Nb at 1200 °C, **h** weld metal with Nb at 1200 °C

Figure 11 shows the microstructure of EGZ for weld metal with and without Nb addition normalized at different temperatures for 2 h. When the normalizing temperatures were 920 and 1020 °C, no WF was observed in the EGZ of the weld metal without and with Nb addition (Fig. 11a–d). The EGZs of both the weld metals—with and without Nb addition—were composed of equiaxed ferrite and pearlite, and the EGZ grain sizes for the weld metal with and without Nb addition were almost equivalent after the 1020 °C normalizing treatment (Fig. 11c, d). When the normalizing temperature was raised to 1120 °C, some WF was found in the EGZ of the Nb-bearing weld metal

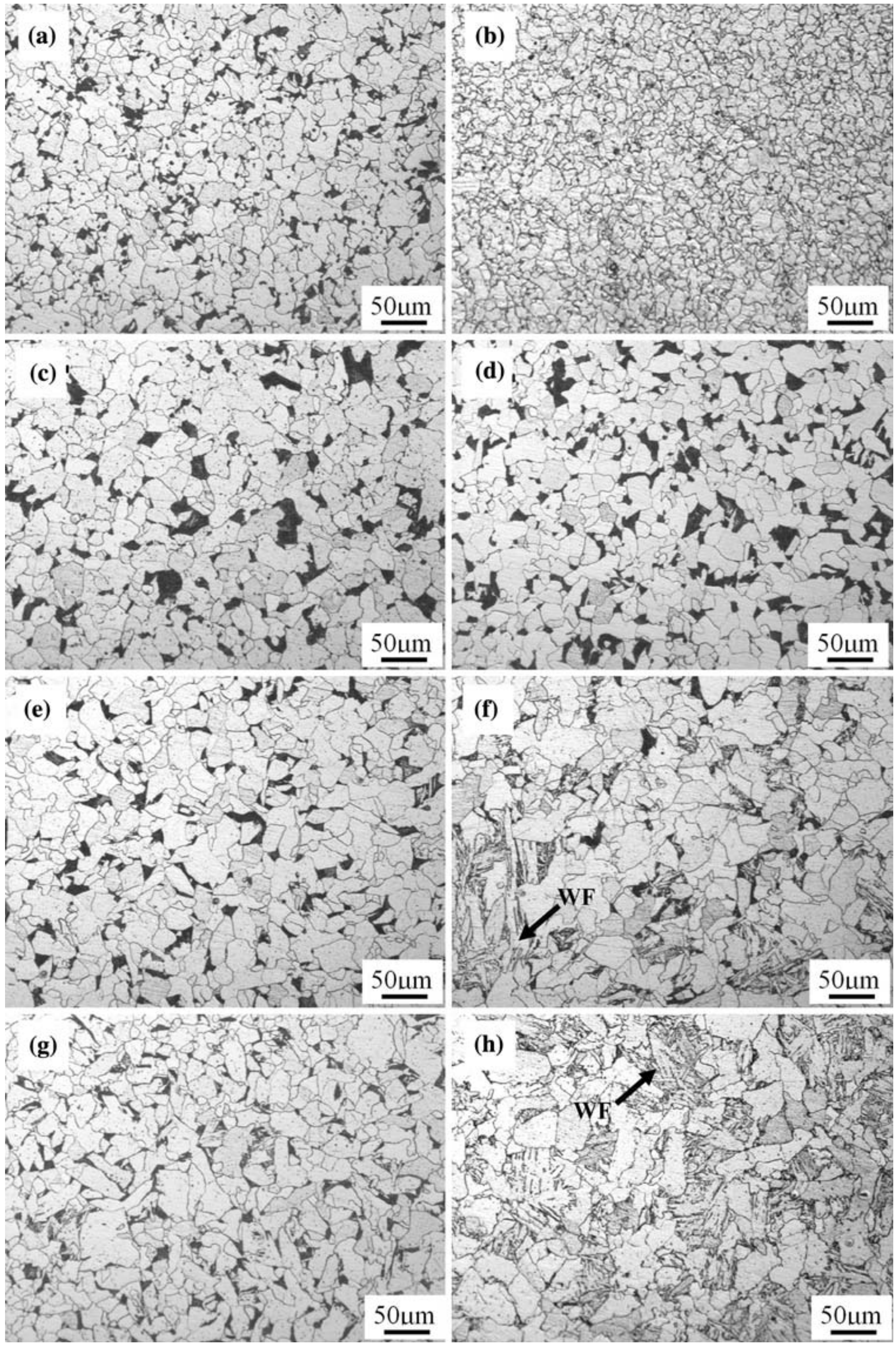

Fig. 11 Microstructure of EGZ for weld metal at different normalizing temperatures for 2 h: **a** weld metal without Nb at 920 °C, **b** weld metal with Nb at 920 °C, **c** weld metal without Nb at 1020 °C, **d** weld metal with Nb at 1020 °C, **e** weld metal without Nb at 1120 °C, **f** weld metal with Nb at 1120 °C, **g** weld metal without Nb at 1200 °C, **h** weld metal with Nb at 1200 °C

(Fig. 11f), while no WF was observed in the EGZ of Nb-free weld metal (Fig. 11e). After normalizing treatment at 1200 °C, almost half of the EGZ in the Nb-bearing weld metal was composed of WF (Fig. 11h), while no WF formed in the EGZ of the Nb-free weld metal (Fig. 11g).

For further analyzing the existing forms of the Nb element in the weld metal under different normalizing conditions. The carbon extraction replicas of the Nb-bearing weld metal under different normalizing conditions were observed using the TEM. The results showed that under the normalizing condition of 920 °C for 2 h, the NbC precipitate size and quantity were larger than those at the as-annealed state as shown in Figs. 12a, b and 7c, d. In a certain temperature range, the size of the NbC precipitates

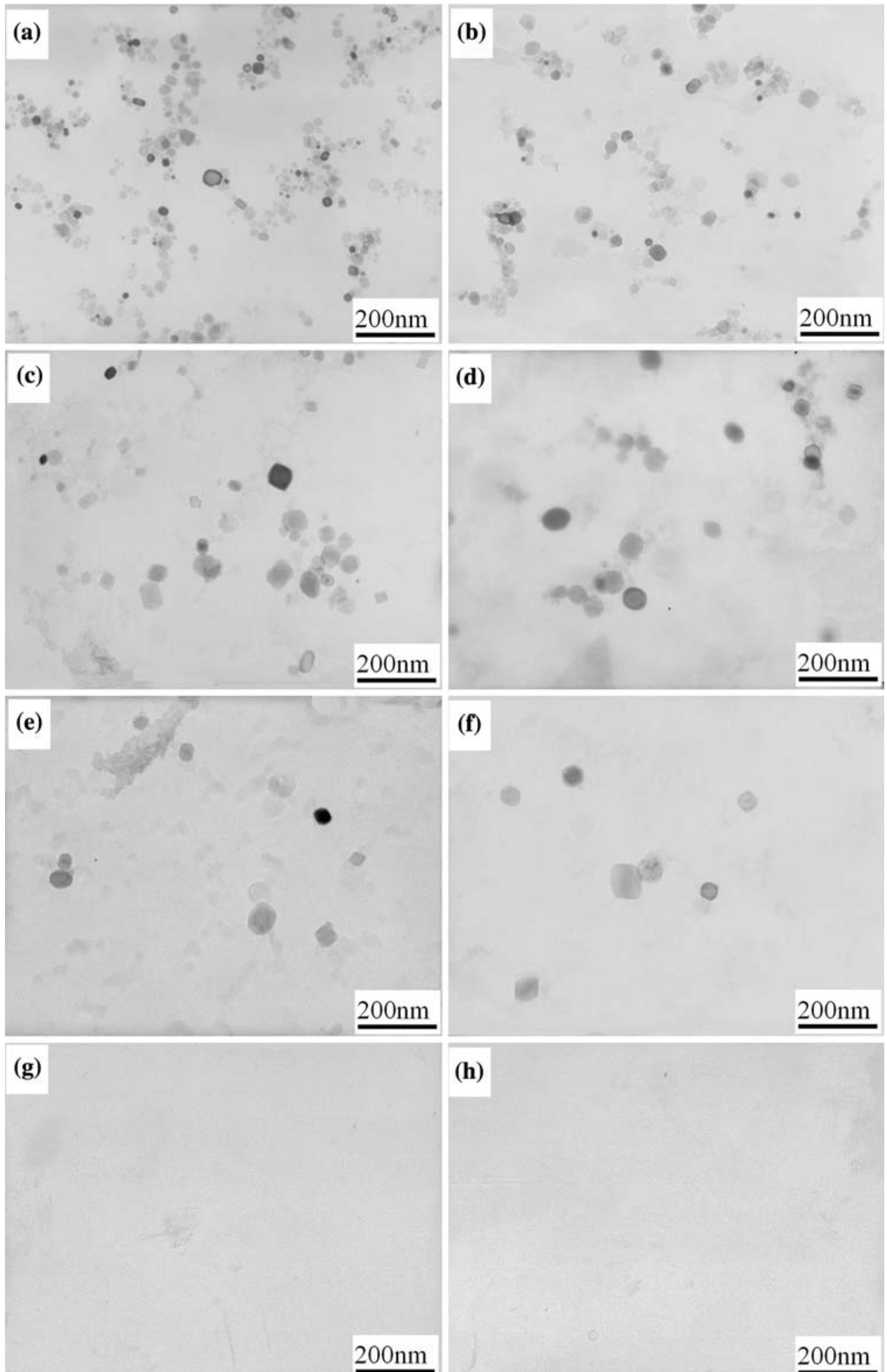

Fig. 12 TEM micrographs of the carbon extraction replica showing NbC in CGZ and EGZ of weld metal with Nb at various normalizing temperatures: **a** CGZ at 920 °C, **b** EGZ at 920 °C, **c** CGZ at 1020 °C, **d** EGZ at 1020 °C, **e** CGZ at 1120 °C, **f** EGZ at 1120 °C, **g** CGZ at 1200 °C, **h** EGZ at 1200 °C

increased, while the quantity of the precipitates decreased with the increase of the normalizing temperature as shown in Fig. 12a–f. Furthermore, when the normalizing temperature was raised to 1200 °C, NbC precipitate was hardly found in the Nb-bearing weld metal as shown in Fig. 12g, h.

Discussion

During the weld metal solidification process, the solute Nb would segregate to the austenite grain boundaries, decrease the grain boundary energy, and suppress the nucleation of

PF at austenite grain boundaries. The strong affinity of Nb and C makes the C diffusion difficult, and lower the advancing rate of austenite and ferrite phase boundaries. The solute drag effect of Nb would also restrain the generation of PF which is formed at higher temperature, and promoting the generation of WF and AF which are formed at lower temperatures [22, 25–27]. This is the reason that small addition of Nb element increases the WF and AF contents and decreases the PF proportion in the CGZ of weld metal (Fig. 6a, b). The increase of WF content would improve the strength of the weld metal, and deteriorate its plasticity and toughness. The increase of AF would improve the strength, plasticity and toughness simultaneously. Under the combined action of WF and AF, the CGZ of the as-welded Nb-bearing weld metal has higher yield and tensile strengths, and elongation comparing with Nb-free weld metal as shown in Tables 4 and 5. EGZ of weld metal experiences the normalizing process by the subsequent welding bead. The EGZ grain size for Nb-bearing weld metal is smaller than that of the Nb-free weld metal due to the grain refining effect of Nb element during the welding process (Fig. 6c, d). Therefore, the EGZ of the as-welded Nb-bearing weld metal has higher yield and tensile strengths and elongation comparing with Nb-free weld metal as shown in Tables 4 and 5.

TEM observation indicated that no precipitate was found in the CGZ of the as-welded Nb-bearing weld metal due to the faster cooling rate after the GMAW welding (Fig. 7a). The NbC precipitates could not form under this cooling condition. The EGZ of the as-welded Nb-bearing weld metal experienced a heat treatment process by the subsequent welding bead, some NbC precipitates formed during the process (Fig. 7b). During the phase transformation process, the precipitated phase NbC can increase nucleation rate of ferrite, promoting grain refinement and improving the mechanical properties of steel. After annealing process, fine NbC precipitates were observed in both the CGZ and EGZ of the Nb-bearing weld metal due to the annealing heat effect (Fig. 7c, d). The lower annealing temperature induced the NbC precipitates formed in the annealing process to be smaller than those formed in the EGZ of the as-welded weld metal (Fig. 7b).

The post-weld annealing process can minimize the residual stress. However, the removal of residual stress is accompanied by carbide spheroidization, carbide formation from enriched profiles in the ferrite, and dislocation recovery. Furthermore, when microalloy elements such as Nb are present in the weld metal, the precipitation of NbC is an additional factor encountered during the annealing process. These microstructural changes during the stress relief annealing process may have opposing effects on the mechanical properties of weld metal [19, 20]. For the Nb-free weld metal, as shown in Table 4, after annealing technology, the yield and tensile strengths decreased, while the elongation and −20 °C impact energy increased, which indicated that the removal of residual stress, carbide spheroidization, and dislocation recovery dominated the properties of the as-annealed Nb-free weld metal [20]. However, for the Nb-bearing weld metal, the annealing process caused the removal of residual stress, carbide spheroidization, and dislocation recovery, but promoted the formation of NbC precipitates, as shown in Fig. 7. After annealing process, for the Nb-bearing weld metal, the yield and tensile strengths increased, while the elongation and −20 °C impact energy decreased, as shown in Table 5, which indicated that the effect of precipitation strengthening was stronger than the influences of removal of residual stress, carbide spheroidization, and dislocation recovery. The NbC precipitates formed during the annealing process dominated the properties of the Nb-bearing weld metal [19].

Optical microstructure (Figs. 8, 9) showed that under the normalizing condition of 920 °C, the microstructures for both the weld metals with and without Nb addition had no obvious change with the different holding times. Therefore, the yield strength, tensile strength, elongation, and −20 °C impact energy of the weld metal with and without Nb addition changed only slightly with the increase of the normalizing holding time at 920 °C as shown in Fig. 3. Furthermore, the mechanical properties of the Nb-bearing weld metal were better than those of the Nb-free weld metal due to the effect of Nb element.

The WF content in the CGZ and EGZ of the Nb-bearing weld metal increased with the increasing normalizing temperature (Figs. 10b, d, f, h and 11b, d, f, h). The formation of WF mainly depends on the chemical composition, austenite grain size, and cooling rate of the steel. When the austenite grain size is coarser and the cooling rate is suitable, PF will be in lamellar morphology and coexisting with lamellar pearlite, and forming the so-called WF. Nb addition can promote the formation of WF in the weld metal. For the CGZ of the Nb-bearing weld metal, after normalizing treatment at 920 °C for 2 h, no WF was found (Fig. 10b). When the normalizing temperature was set at 1020 °C, some austenite grains in the CGZ of the Nb-bearing weld metal met the WF formation condition, and transformed into WF finally (Fig. 10d). More WF formed in the CGZ of the Nb-bearing weld metal with the increase of the normalizing temperature (Fig. 10f, h). When the normalizing temperature was raised to 1200 °C, most of the austenite grains in the CGZ of the Nb-bearing weld metal became coarser and satisfied the WF formation condition. Eventually, the majority of the weld metal changed into WF, the others converted into equiaxed ferrite (Fig. 10h). However, for the CGZ of the Nb-free weld metal, only when the normalizing temperature was 1200 °C, a few austenite grains in the CGZ of the Nb-free weld metal satisfied the WF formation condition and transformed into WF (Fig. 10g). For the EGZ for weld metal with and without Nb addition after normalizing at different temperatures for 2 h, similar results as the CGZ could be obtained for the same reasons (Fig. 11).

The increase of the WF content in the Nb-bearing weld metal would improve the strength and deteriorate the elongation and impact energy of the weld metal. Therefore, for the weld metal containing Nb element, with the increase of the normalizing temperature, the yield and tensile strengths increased obviously (Fig. 4a, b), while the elongation and −20 °C impact energy decreased significantly (Fig. 4c, d).

TEM observation of the NbC precipitates in the Nb-bearing weld metal under different normalizing conditions indicated that the NbC precipitates were apt to grow up at higher temperatures within a certain temperature range (Fig. 12). However, when the normalizing temperature was raised to 1200 °C, NbC precipitate was hardly found in the Nb-bearing weld metal as shown in Fig. 12g, h. The NbC precipitates would dissolve into the substrate when the normalizing temperature exceeded the solid solution temperature of NbC, which was below 1200 °C suggested by literatures [28, 29].

Conclusions

1. In the as-welded state, the Nb-free weld metal has lower yield and tensile strengths, elongation, and equivalent −20 °C impact energy compared with those of the Nb-bearing weld metal. After stress relief annealing, for the Nb-free weld metal, the yield and tensile strengths decrease, the elongation, and −20 °C impact energy increase. However, for the Nb-bearing weld metal, the yield and tensile strengths increase, while the elongation and −20 °C impact energy decrease.
2. The Nb addition promotes the formation of WF and AF, and restrains the formation of PF in the weld metal. In the CGZ of the as-welded Nb-bearing weld metal, no NbC precipitate was found. After annealing process, NbC precipitates were found in CGZ of the weld metal. The NbC precipitates improved the strength of the weld metal, whereas they caused deterioration in its plasticity and toughness.
3. With the increase of the holding time at the normalizing temperature of 920 °C, there are no significant changes in the optical microstructure, so that the mechanical properties of the weld metal with and without Nb addition remain almost unchanged.
4. The content of WF in the Nb-bearing weld metal increases obviously with the increase of the normalizing temperature, which makes the yield and tensile strengths increased obviously, while the elongation and −20 °C impact energy decreased significantly. Furthermore, the quantity of the NbC particles in the Nb-bearing weld metal decreases as the normalizing temperature increases, and finally dissolving into the substrate as the normalizing temperature reaches 1200 °C.

Acknowledgements The authors are grateful for the financial support from the National Key Technologies R&D Program of China under Grant No. 2009BAG12A07-D06 and National Science Foundation of China (NSFC) under Grant No. 50874101.

References

1. Zhang YQ, Zhang HQ, Liu WM, Hou H (2009) Mater Sci Eng A 499:182
2. Pereloma EV, Timokhina IB, Russell KF, Miller MK (2006) Scr Mater 54:471
3. Beladi H, Hodgson PD (2007) Scr Mater 56:1059
4. Thridandapani RR, Misra RDK, Mannering T, Panda D, Jansto S (2006) Mater Sci Eng A 422:285
5. Park JS, Lee YK (2007) Scr Mater 57:109
6. Lee SJ, Lee YK (2005) Scr Mater 52:973
7. Zhang ZH, Liu YN, Liang XK, She Y (2008) Mater Sci Eng A 474:254
8. Shanmugam S, Misra RDK, Hartmann J, Jansto SG (2006) Mater Sci Eng A 441:215
9. Yu QB, Wang ZD, Liu XH, Wang GD (2004) Mater Sci Eng A 379:384
10. Shanmugam S, Ramisetti NK, Misra RDK, Mannering T, Panda D, Jansto S (2007) Mater Sci Eng A 460–461:335
11. Anumolu R, Ravi Kumar B, Misra RDK, Mannering T, Panda D, Jansto SG (2008) Mater Sci Eng A 491:55
12. Shanmugam S, Ramisetti NK, Misra RDK, Hartmann J, Jansto SG (2008) Mater Sci Eng A 478:26
13. Reip CP, Shanmugam S, Misra RDK (2006) Mater Sci Eng A 424:307
14. Shanmugam S, Misra RDK, Mannering T, Panda D, Jansto SG (2006) Mater Sci Eng A 437:436
15. Pereloma EV, Timokhina IB, Hodgson PD (1999) Mater Sci Eng A 273–275:448
16. Nayak SS, Misra RDK, Hartmann J, Siciliano F, Gray JM (2008) Mater Sci Eng A 494:456
17. Shiga C, Gotoh A, Kojima T, Horii Y, Fukada Y, Ikeuti K, Matuda F (1996) Weld World 37:163
18. Billy J, Johansson T, Loberg B, Easterling KE (1980) Met Technol 7:67
19. Farrar RA, Ferrante M (1982) J Mater Sci 17:2405. doi:10.1007/BF00543751
20. Farrar RA, Taylor LG, Harrison EM (1979) Met Technol 6:380
21. Garland JG, Kirkwood PR (1975) Met Constr 7:275
22. Farrar RA, Wong SY, Watson MNW (1980) Weld Met Fabr 48:21
23. Enterkin CH (1983) Weld J 62:197s
24. Garland JG, Kirkwood PR (1975) Met Constr 7:320
25. Yi HL, Du LX, Wang GD, Liu XH (2005) J Mater Metall 4:295 (In Chinese)
26. Lee KJ, Lee JK, Kang KB, Kwon O (1992) ISIJ Int 32:326
27. Manohar PA, Chandra T, Killmore CR (1996) ISIJ Int 36:1486
28. Hong SC, Lim SH, Hong HS, Lee KJ, Shin DH, Lee KS (2003) Mater Sci Eng A 355:241
29. Li Y, Wilson JA, Crowther DN, Mitchell PS, Craven AJ, Baker TN (2004) ISIJ Int 44:1093